Synthesis of an Anthraquinone-Bridged bis(terpyridine) Ligand and its Use in the Stepwise Fabrication of Complex Oligomer Wires on Gold

*Mitsuya Utsuno, Fumiyuki Toshimitsu, Shoko Kume, Hiroshi Nishihara**

Summary: A new bis(terpyridine) ligand with an anthraquinone linker was synthesized. Stepwise coordination reactions at the gold surface using this ligand gave homo-metal oligomer wires up to pentamer, **[*n*FeL$_1$]** ($n = 1$–5), and hetero-metal oligomer wires with ferrocene as the terminal group, **[1FeL$_1$1FeL$_2$Fc]**. Electrochemical properties of these modified electrodes were examined.

Keywords: anthraquinone; bis(terpyridine) ligand; cyclic voltammogram; electrochemistry; ferrocene; iron complex

Introduction

Modification of an electrode substrate by adsorption and immobilization of functional molecules is a significant factor in the creation of molecular devices.[1–4] Self-assembled-monolayers (SAMs)[5–7] have been widely used as the modification, and construction of multi-layer structures using reactions on the solid surface have been reported in recent years.[8–11] Moreover, these layer-by-layer structures are expected to be applied to the construction of nano-scale devices such as dye-sensitized solar cells and organic light-emitting diodes.

We have reported the preparation and immobilization of one-dimensional transitional metal complex oligomer by using stepwise complexation on a gold electrode surface, a "bottom-up method".[12–14] In addition, based on observation of the electron transfer of the complex wire, intrachain stepwise electron transfer between redox sites has been determined.[14]

The electron transfer kinetics between redox sites is thought to depend on the structure and properties of bridging ligands; in particular, the structure of the bridging moiety is thought to influence the electron transfer ability of the complex wire. Herein, I describe preparation of new complex wire using bridging ligand, **L$_1$**, with two terpyridine moieties being bound to the 1,4-position of anthraquinone through a triple bond. The wires are homo-complex oligomer wires up to pentamer, **[*n*FeL$_1$]** ($n =$ 1–5), and hetero-complex oligomer wires with ferrocene as the terminal group, **[1FeL$_1$1FeL$_2$Fc]** (Figure 1). Electrochemical analysis of the wires and IR characterization of the surface films are described in this paper, as well as observation of the electron transfer of the complex wire.

Experimental Part

General

4′-Ethynyl-2,2′;6′,2″-terpyridine,[15] **(tpy-AB-S)$_2$**,[13] 1,4-dibromoanthraquinone,[16] and 4′-(ferrocenylethynyl)-2,2′;6′,2″-terpyridine (**L$_2$Fc**)[17] were synthesized according to literature methods. Other reagents were obtained from commercial sources and used as received. Water for preparation of films was purified by passage through a Milli-Q purification system (Millipore).

^{1}H NMR spectra were measured with a Bruker DRX 500 (500 MHz) spectrometer. MALDI-TOF mass spectra were measured with a Shimadzu/KRATOS AXIMA-CFR

Department of Chemistry, School of Science, The University of Tokyo, Tokyo 113-0033, Japan
E-mail: nishihara@chem.s.u-tokyo.ac.jp

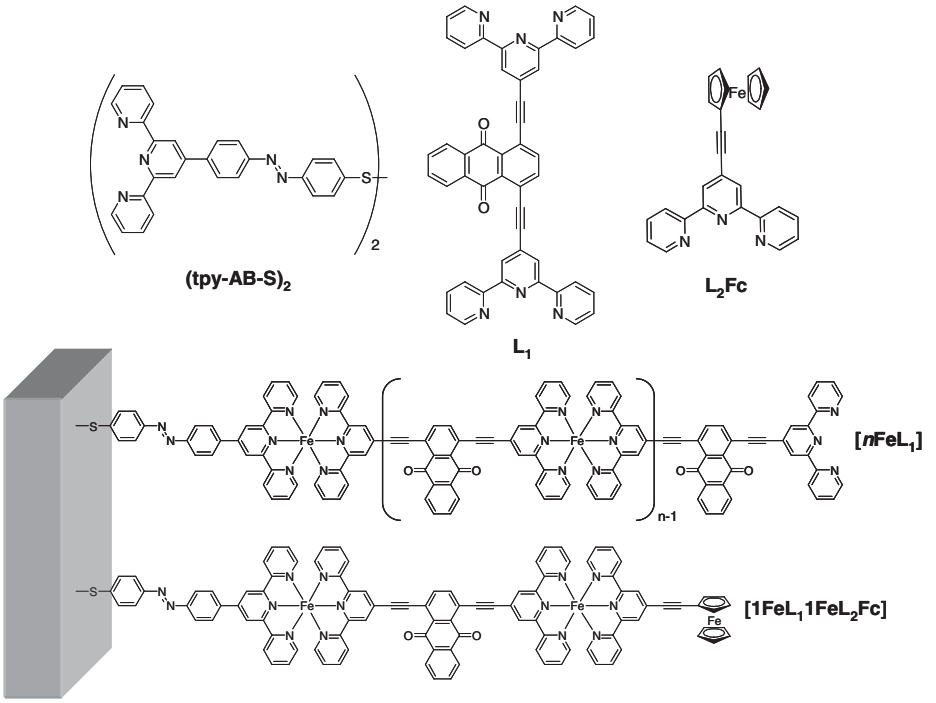

Figure 1.
Structures of ligands for preparing complex wires and constructed complex wires.

time-of-flight mass spectrometer. IR spectra in the KBr pellet were measured with a JASCO FT/IR-620v spectrometer, and surface RAS-IR spectra were measured under vacuum at an incident angle of 85° with a JASCO FT/IR-6300 type A. Electrochemical measurements were carried out in a one-compartment cell with a Au/mica working electrode, a Pt wire counter electrode, and an Ag/Ag^+ reference electrode under Ar with an ALS-750A and an ALS-650B analyzer (BAS Co., Ltd.).

Syntheses

1,4-Bis[2,2′;6′,2″]terpyridin-4′-yl-ethynyl-anthraquinone (L1)

1,4-Dibromoanthraquinone (0.20 g, 0.55 mmol), 4′-ethynyl-2,2′;6′,2″-terpyridine (0.28 g, 0.55 mmol), CuI (8 mg, 0.04 mmol), and $Pd(PPh_3)_4$ (13 mg, 0.01 mmol) were dispersed in triethylamine (60 ml) and heated to reflux for 16 h. The color of the reaction mixture turned from yellow to yellowish green. The solvent was removed under vacuum. After solvent removal, the crude product was chromatographed on an alumina column (activity III) with dichloromethane. The second yellowish-brown fraction was collected, the solvent was evaporated, and the residue was then reprecipitated from dichloromethane-acetonitrile to afford a yellow solid (0.13 g, 32%). ^{1}H NMR (500 MHz, $CDCl_3$): δ 8.76 (dd, $J = 3.9$, 1.0 Hz, 4H); 8.75 (s, 4H); 8.66 (d, $J = 7.9$ Hz, 4H); 8.38 (dd, $J = 7.1$, 3.9 Hz, 2H); 8.02 (s, 2H); 7.92 (td, $J = 4.4$, 1.7 Hz, 4H); 7.85 (dd, $J = 5.9$, 2.7 Hz, 2H); 7.39 (ddd, $J = 7.6$, 3.9, 1.2 Hz, 4H). IR (KBr, cm^{-1}) 2209 (w), 1675. Anal. Calcd. for $C_{48}H_{26}N_6O_2 \cdot 3/4H_2O$: C, 78.73; H, 3.79; N, 11.48. Found: C, 79.09; H, 3.97; N, 11.06. MALDI-TOF MS: 719.05 ($C_{48}H_{26}N_6O_2$ + 1H requires 719.21).

Preparation of Fe complex oligomer ([L1 + Fe] oligomer) in solution

L_1 (3.5 mg) was dissolved in chloroform (50 ml), and a 0.1 M aqueous solution of

$Fe(BF_4)_2$ (about 0.1 ml, excess) was added to the L_1 solution and stirred at room temperature for 3 days. The reaction mixture turned from yellowish-green solution to blue-purple suspension, and precipitation occured. The precipitate was collected and washed with chloroform, water, and ethanol to afford a blue-purple solid.

Stepwise Preparation of Complex Wires on Au

Au/mica plates (gold (100 nm) deposited on natural mica) were annealed with a hydrogen frame, and a Au(111) surface was created just before use. First, the plates were immersed in a 0.1 mM chloroform solution of **(tpy-AB-S)$_2$** for 5 min, washed with HPLC grade chloroform, and dried with nitrogen blow. The plates were then immersed in a 0.1 M aqueous solution of $Fe(BF_4)_2$ for 2 h, washed with water and ethanol, and dried with nitrogen blow. The plates were immersed in a 0.1 mM chloroform solution of **L_1** for a given period, washed with chloroform, and dried with nitrogen blow. For preparation of oligomeric film ($n \geq 2$), these last two processes (immersion in $Fe(BF_4)_2$ solution and then bridging ligand solution) were repeated (see Figure 2).

Films of ferrocene-terminated complex wire, **[1FeL$_1$1FeL$_2$Fc]**, were prepared using the procedures to prepare **[*n*FeL$_1$]** noted above and a ferrocene-terminated terpyridine ligand, **L$_2$Fc**. After preparation of **[1FeL$_1$]**, the plate was immersed in 0.1 M aqueous solution of $Fe(BF_4)_2$ for 3 h, washed with water and ethanol, and dried with nitrogen blow. The plate was then immersed in 0.1 mM chloroform solution of **L$_2$Fc** for 24 h, washed with chloroform, and dried with nitrogen blow.

Results and Discussion

Preparation of Monolayer, [1FeL$_1$], and its Redox Properties

The immersion time dependence in **L_1** solution was first examined for the most suitable and efficient preparation conditions. Figure 3 shows cyclic voltammograms of monolayer films, **[1FeL$_1$]**, when the

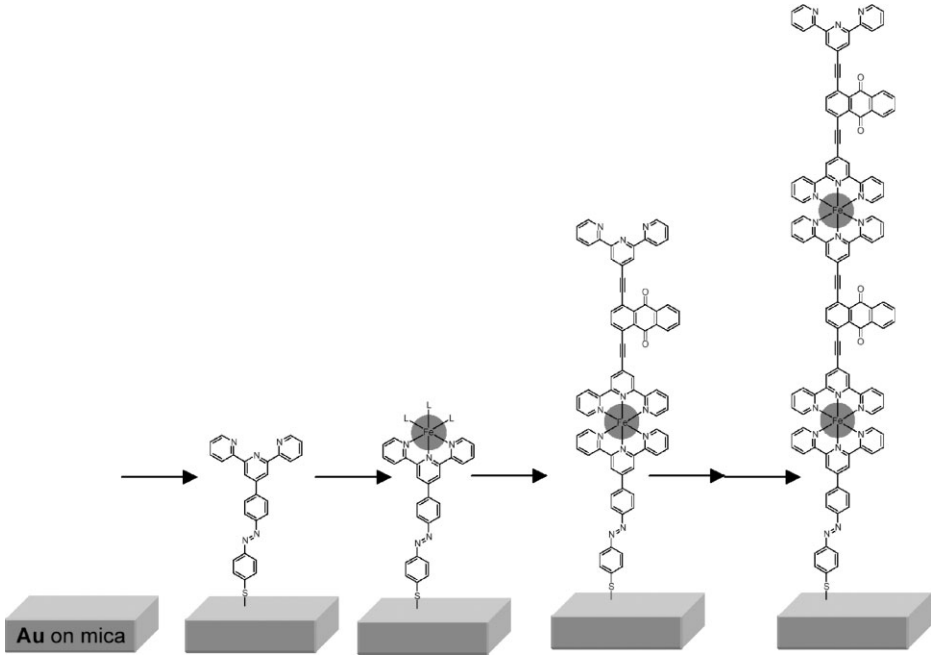

Figure 2.
Schematic image of preparing **[*n*FeL$_1$]** complex wire.

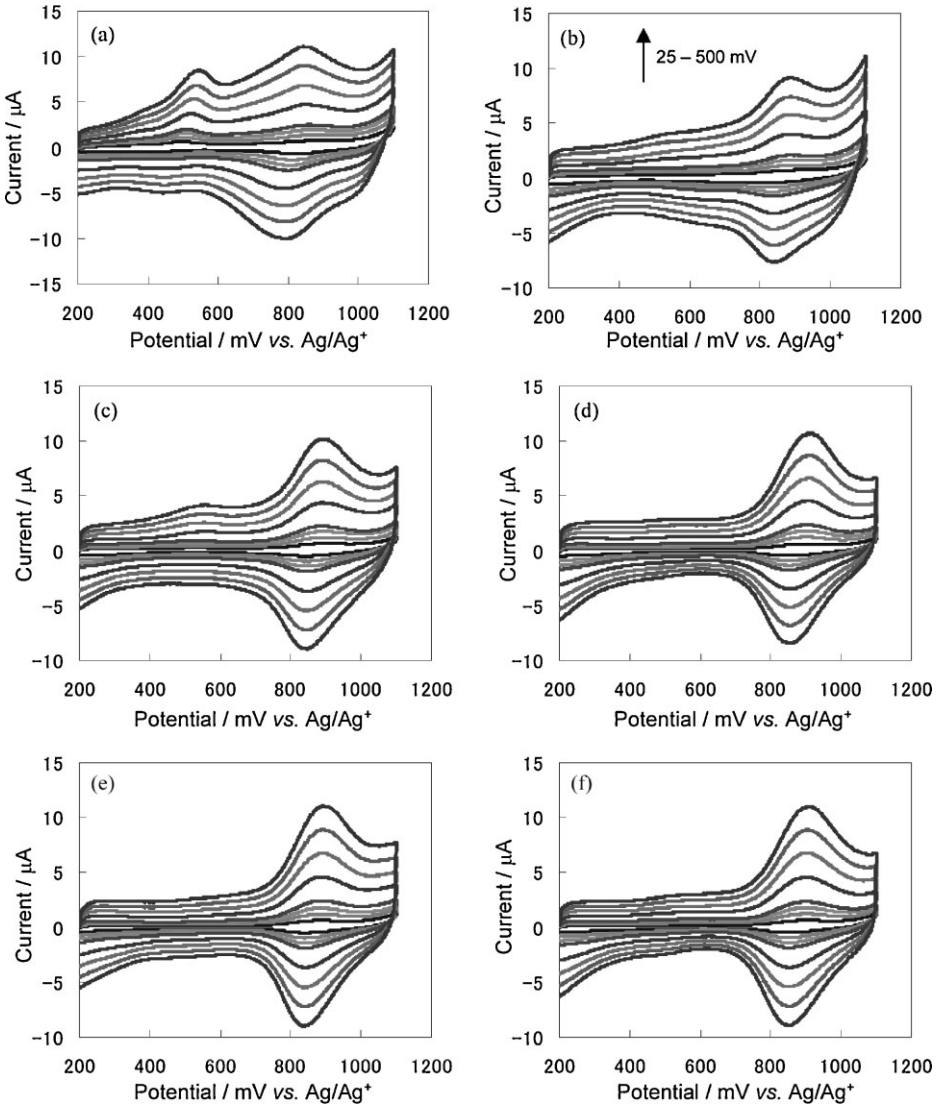

Figure 3.
Cyclic voltammograms of **[1FeL$_1$]** in 0.1 M Bu_4NClO_4-CH_2Cl_2 with immersion times in $\mathbf{L_1}$ solution of (a) 5 min, (b) 30 min, (c) 60 min, (d) 2 h, (e) 24 h, and (f) 48 h. The scan rates were 25, 50, 75, 100, 200, 300, 400, and 500 mVs^{-1}.

immersion time was changed from 5 min to 48 h. In all the voltammograms, reversible redox waves appeared around 0.85 V *vs.* Ag/Ag^+, which can be ascribed to the reaction of the $[Fe(tpy)_2]^{3+/2+}$ redox couple. In the cyclic voltammogram of the 5-min-immersion film, not only the $[Fe(tpy)_2]^{3+/2+}$ redox wave, but also an irreversible oxidation wave was observed around 0.60 V. This peak decreased with increases in the immersion time, and was hardly observed for the 60-min immersion film. From these results, this irreversible peak can be attributed to a quasi-stable state, although the exact structure in this state has not yet been clarified. Figure 4 displays the plots of peak potential, E_{pa} and E_{pc}, and the formal potential, $E^{0'} = (E_{pa} + E_{pc})/2$ for the $[Fe(tpy)_2]^{3+/2+}$ redox couple (scan rate was 0.1 Vs^{-1}) vs. the immersion

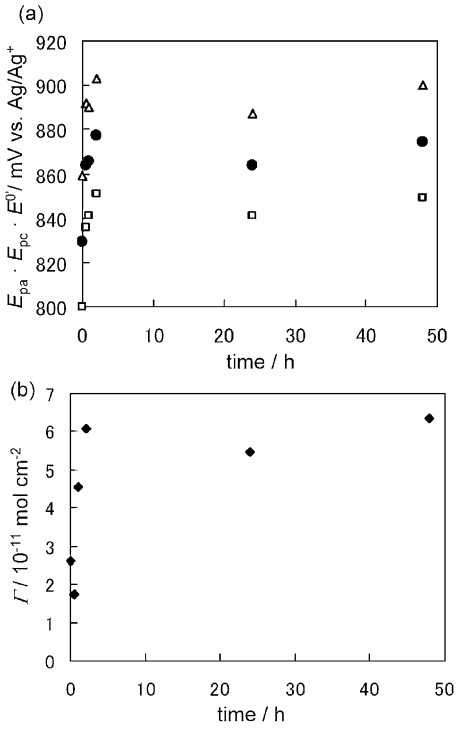

Figure 4.
Plots of E_{pa} (triangle), E_{pc} (square), and $E^{o'}$ (circle) for the $[Fe(tpy)_2]^{3+/2+}$ redox couple vs. the immersion time (a), and plots of surface coverage of the redox active sites vs. the immersion time in preparing **[1FeL$_1$]** (b).

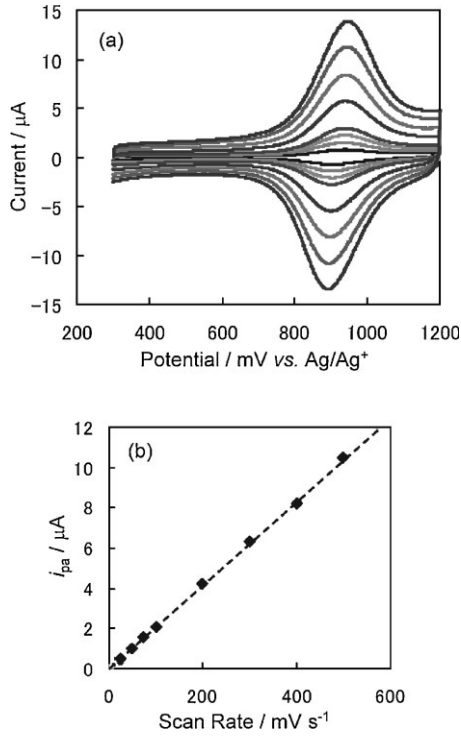

Figure 5.
Cyclic voltammograms of **[1FeL$_1$]** (prepared with an immersion time of 1 day in L1 solution) in 1 M Bu_4NClO_4/CH_2Cl_2 at scan rates of 25, 50, 75, 100, 200, 300, 400, and 500 mVs^{-1} (a), and plots of anodic peak current *vs.* the scan rate (b).

time, and the plots of surface coverage of the redox active sites, Γ, estimated from the amount of charge passed during the redox reaction *vs.* the immersion time. The surface coverage increased initially until 2 h of immersion time, while it remained almost constant for further immersion, indicating that complex formation on the electrode surface was accomplished in a few hours. In addition, a correlation between $E^{0'}$ and surface coverage can be observed in Figure 4, implying that the concentrations of the redox sites on the surface influence the thermodynamics of the redox reaction, as has been reported in other redox monolayer electrode films.[18]

Cyclic voltammograms of **[1FeL$_1$]** prepared under the conditions mentioned above are shown in Figure 5a, where a reversible oxidation wave attributed to the reaction of $[Fe(tpy)_2]^{3+/2+}$ redox couple can be observed at 0.90 V vs. Ag/Ag^+. Plots of scan rate vs. peak current, i_{pa}, in Figure 5b show that the peak current is proportional to the scan rate, supporting the redox reaction of surface-immobilized species. The Γ value estimated from the amount of charge passed during the oxidation reaction was $1.1 \pm 0.2 \times 10^{-10}$ mol cm^{-2}, which is similar to the values for the films with tpy-C_6H_4-N=N-C_6H_4-tpy[12] ($\Gamma = 1.4 \times 10^{-10}$ mol cm^{-2}) or tpy-C_6H_4-tpy ($\Gamma = 1.0 \times 10^{-10}$ mol cm^{-2}).[14]

Preparation of Homo-Metal Multilayers, [nFeL$_1$], and their Redox Properties

The conditions suitable to preparing oligomeric complex wires by repeating immersion in a $Fe(BF_4)_2$ solution and a **L$_1$** solution were examined next. When the second

layer formation was carried out under the same condition as that for the 1st layer, that is the immersion time in a solution of $\mathbf{L_1}$ was 2 h, little increase in the peak current for the $[Fe(tpy)_2]^{3+/2+}$ redox couple, and, accordingly, little surface coverage were observed (Figure 6). We then examined the dependency of the surface coverage of electroactive sites in **[1FeL$_2$]** on the immersion time in a $\mathbf{L_1}$ solution for the second layer formation, and the results are given in Figure 6 (for 48 h) and Figure 7. Figure 7 indicates that saturation of $Fe(tpy)_2$ complex formation in the 2nd layer is slower than in the 1st layer, taking more than 16 h. This period is much longer compared with cases using another bridging ligand such as tpy–C_6H_4–N=N–C_6H_4-tpy[12] or tpy-C_6H_4-tpy.[14] This difference is likely due to the electron-withdrawing effect and the bulkiness of the anthraquinone moiety in $\mathbf{L_1}$, leading to slower kinetics in complex formation. Based on these results, we carried out stepwise complex layer formation using 1 day as the immersion time in a $\mathbf{L_1}$ solution after the 2nd layer.

Figure 8a shows cyclic voltammograms of the **[*n*FeL$_1$]** wires ($2 \leq n \leq 5$). The current quantities increased as n increased. The proportional relationship between i_{pa} and the scan rate shown in Figure 8b indicates that these oxidation waves were all attributed to electroactive species immobilized on the gold electrode. Γ values were estimated from the cyclic voltammograms and plotted against the number of layers, n,

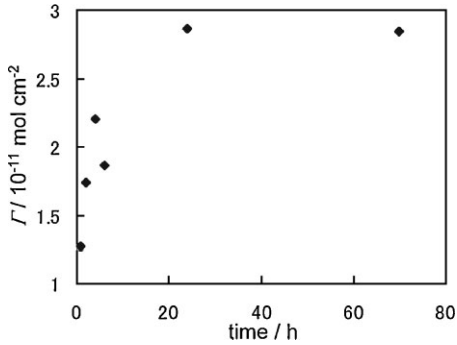

Figure 7.
Plots of surface coverage *vs.* immersion time in preparing **[2FeL$_1$]**.

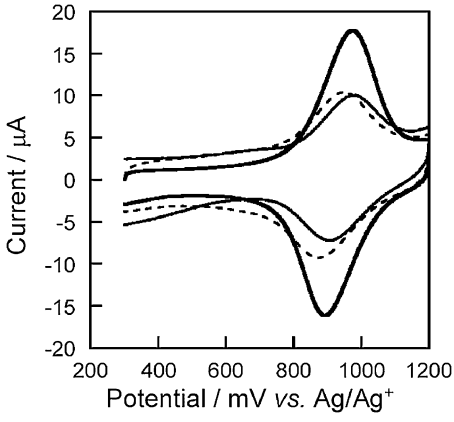

Figure 6.
Cyclic voltammograms at 0.1 Vs^{-1} of **[1FeL$_1$]** (solid line), **[1FeL$_1$]** + $Fe(BF_4)_2$ + $\mathbf{L_1}$ (immersing for 2 h) (dashed line), and **[1FeL$_1$]** + $Fe(BF_4)_2$ + $\mathbf{L_1}$ (immersing for 48 h) (bold line) in 0.1 M Bu_4NClO_4-CH_2Cl_2.

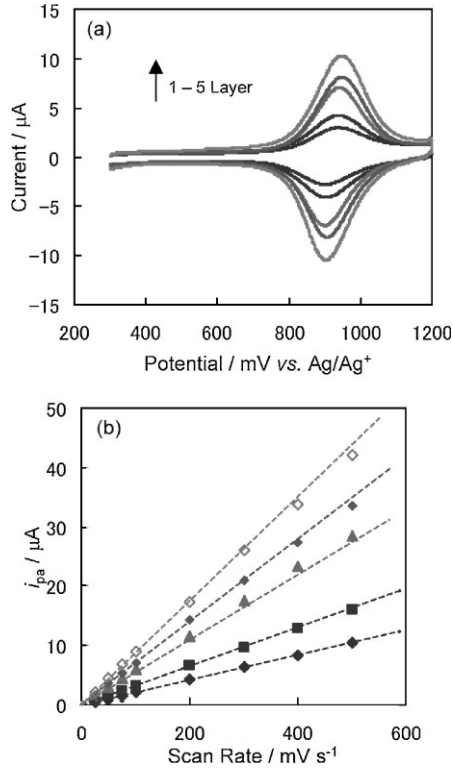

Figure 8.
Cyclic voltammograms of **[*n*FeL$_1$]** ($n = 1$–5) at a scan rate of 0.1 Vs^{-1} in 1 M Bu_4NClO_4-CH_2Cl_2 (a), and plots of anodic peak current vs. scan rate (b).

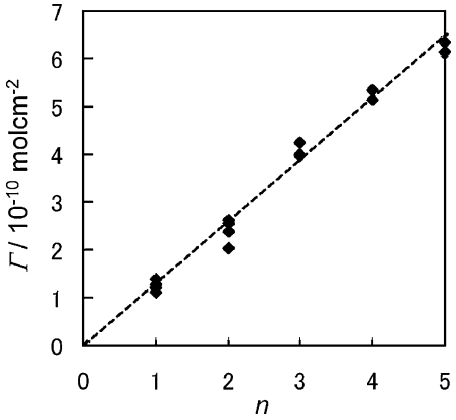

Figure 9.
Plots of surface coverage *vs.* the number of complexation cycles for **[*n*FeL$_1$]**.

as shown in Figure 9. Surface coverage was proportional to n, and thus almost perfect construction of a one-dimensional complex oligomer by using $\mathbf{L_1}$ was accomplished.

Figure 10 shows IR spectra of $\mathbf{L_1}$, **[$\mathbf{L_1}$ + Fe]** oligomer prepared in solution, and a **[3FeAQ]** film on Au. The **[3FeAQ]** film exhibited absorption around 1700 cm^{-1} attributed to the C=O stretching vibration, as observed in $\mathbf{L_1}$ and **[$\mathbf{L_1}$ + Fe]** oligomer. A broad absorption around 1000 cm^{-1} originated from BF_4^{--}, indicating that BF_4^{--} anions were including in this film. In addition, absorption peaks in the region of 1200-1600 cm^{-1} were identical to those of **[$\mathbf{L_1}$ + Fe]** oligomer. These results, together with the electrochemical ones described above, confirm the construction of complex oligomer wires with $\mathbf{L_1}$ bridges.

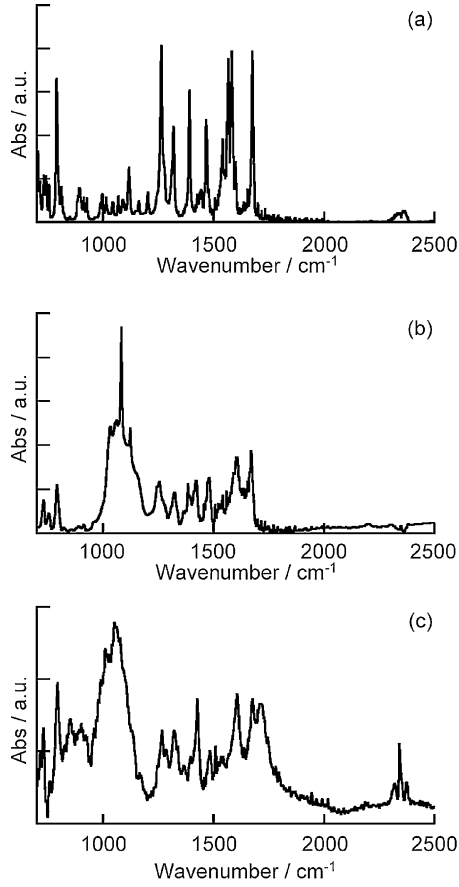

Figure 10.
IR spectra of $\mathbf{L_1}$ in KBr pellet (a), **[$\mathbf{L_1}$ + Fe]** oligomer in KBr pellet (b), and **[3FeAQ]** film on Au/mica (c)

Preparation of Hetero-Nuclear Multilayers, [1FeL$_1$1FeL$_2$Fc], and their Redox Properties

A cyclic voltammogram of **[1FeL$_1$1FeL$_2$Fc]** is shown in Figure 11. A reversible oxidation wave was observed at 0.28 V *vs.* Ag/Ag^+, which can be attributed to the ferrocenium/ferrocene couple at the terminal of the molecular wire, judging from the formal potential. When the potential scan range was extended to + 1.2 V to observe the redox reaction of $[Fe(tpy)_2]^{3+/2+}$, a rapid decrease in the redox activity of the ferrocene moieties was observed, while the activity was maintained without experience of the $[Fe(tpy)_2]^{3+/2+}$ redox reaction for several tens of scans at 0.1 Vs^{-1}. Surface immobilization of the ferrocene moieties was confirmed by the i_{pa} vs. scan rate plots, and surface coverage of ferrocene moieties, Γ_{Fc}, evaluated from the amount of charge passed during the redox reaction was 5.6×10^{-11} mol cm^{-2}. This Γ_{Fc} value was approximately 50% of the Γ value for the $Fe(tpy)_2$ moieties in one layer, 1.1×10^{-10} mol cm^{-2} (*vide supra*), indicating that approximately half of the terpyridine sites of fabricated **[1FeL$_1$]** were connected with $\mathbf{L_2Fc}$. This result is thought to be due to the steric hindrance of the ferrocene moiety, as

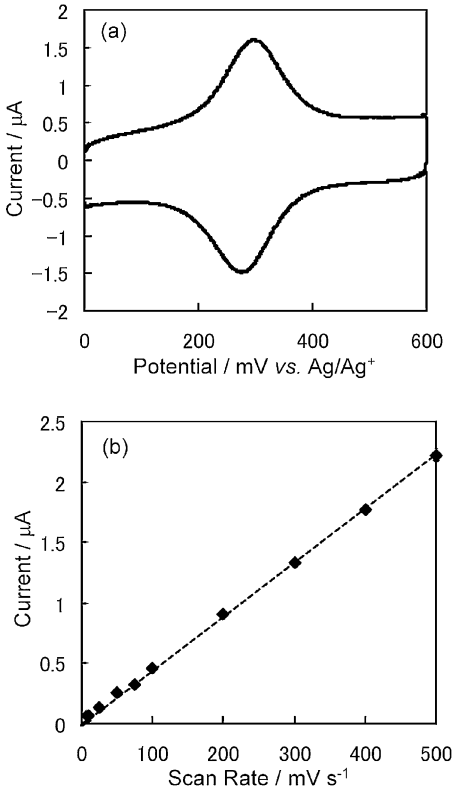

Figure 11.
Cyclic voltammogram of **[1FeL$_1$1FeL$_2$Fc]** at a scan rate of 0.1 Vs^{-1} in 1 M Bu_4NClO_4-CH_2Cl_2 (a), and plots of anodic peak current vs. scan rate (b).

demonstrated in the crystal structure of Zn(L_2Fc) reported by Siemeling et al.[7]

Conclusion

A new terpyridine ligand with an anthraquinone linker, **L$_1$**, was synthesized and utilized to construct redox-active homo- and hetero-complex wires, **[*n*FeL$_1$]** ($n = 1$–5) and **[1FeL$_1$1FeL$_2$Fc]**, respectively, fixed on the gold electrode surface by using the complexation of ferrous ion and terpyridine. The complexation depends on the immersion time in a solution of **L$_1$**, and adequate conditions for the complexation could achieve almost perfect elongation of the molecular wires. A hetero-complex wire **[1FeL$_1$1FeL$_2$Fc]** prepared by the stepwise coordination method exhibited a reversible redox reaction of the ferrocene moieties accounting for approximately half of the pre-constructed **[1FeL$_1$1Fe]** molecular wires.

Acknowledgements: This work was supported by Grants-in-Aid for Scientific Research (Nos. 16047204 (area 434) and 17205007), by a grant from The 21st Century COE Program for Frontiers in Fundamental Chemistry from MEXT, and by CREST, JST, Japan.

[1] C. Joachim, J. K. Gimzewski, A. Aviram, *Nature* **2000**, *408*, 541.
[2] J. Park, A. N. Pasupathy, J. I. Goldsmith, C. Chang, Y. Yaish, J. R. Petta, M. Rinkosiki, J. P. Sethna, H. D. Abruña, P. L. McEuen, D. C. Ralph, *Nature* **2002**, *417*, 722.
[3] C. E. D. Chidsey, R. W. Murray, *Science* **1986**, *231*, 25.
[4] M. S. Wrighton, *Science* **1986**, *231*, 32.
[5] B. Vercelli, G. Zotti, A. Berlin, S. Grimoldi, *Chem. Mater.* **2006**, *18*, 3754.
[6] S. Zhang, A. Palker, L. Echegoyen, *Langmuir* **2006**, *22*, 10732.
[7] M. Hölzl, A. Tinazli, C. Leitner, C. D. Hahn, B. Lackner, T. Tampé, H. J. Gruber, *Langmuir* **2007**, *23*, 5571.
[8] G. K. Such, J. F. Quinn, A. Quinn, E. Tjipto, F. Caruso, *J. Am. Chem. Soc.* **2006**, *128*, 9318.
[9] J. Jiao, F. Anariba, H. Tizanado, I. Schmidt, J. S. Lindsey, F. Zaera, D. F. Bocian, *J. Am. Chem. Soc.* **2006**, *128*, 6965.
[10] M. Wanunu, A. Vaskevich, A. Shanzer, I. Rubinstein, *J. Am. Chem. Soc.* **2006**, *128*, 8341.
[11] M. Abe, T. Michi, A. Sato, T. Kondo, W. Zhou, S. Ye, K. Uosaki, Y. Sasaki, *Angew. Chem. Int. Ed.* **2003**, *42*, 2912.
[12] K. Kanaizuka, M. Murata, Y. Nishimori, I. Mori, K. Nishino, H. Masuda, H. Nishihara, *Chem.Lett.* **2005**, *34*, 534.
[13] Y. Ohba, K. Kanaizuka, M. Murata, H. Nishihara, *Macromol. Symp.* **2006**, *235*, 31.
[14] Y. Nishimori, K. Kanaizuka, M. Murata, H. Nishihara, *Chem. Asian J.* **2007**, *2*, 367.
[15] V. Grosshenny, F. R. Romero, R. Ziesell, *J. Org. Chem.* **1997**, *62*, 1491.
[16] M. P. Doyle, B. Siegfried, J. F. Dellaria, Jr., *J. Org. Chem.* **1977**, *42*, 2426.
[17] U. Siemeling, J. V. Brüggen, U. Vorfeld, B. Neumann, A. Stammler, H.-G. Stammler, A. Brockhinke, R. Plessow, P. Zanello, F. Laschi, F. F. Biani, M. Fontani, S. Steenken, M. Stapper, G. Gurzadyan, *Chem. Eur. J.* **2003**, *9*, 2819.
[18] J. Petrovic, R. A. Clark, H. J. Yue, D. H. Waldeck, E. F. Bowden, *Langmuir* **2005**, *21*, 6308.

